

RESEARCH ARTICLE | JANUARY 15 1990

Strain mapping in [111] and [001] InGaAs/GaAs superlattices



U. D. Venkateswaran; L. J. Cui; M. Li; ... et. al



Appl. Phys. Lett. 56, 286–288 (1990)

<https://doi.org/10.1063/1.102810>



CrossMark

Articles You May Be Interested In

In situ measurements of critical layer thickness and optical studies of InGaAs quantum wells grown on GaAs substrates

Appl. Phys. Lett. (October 1989)

Zn-diffused laser junctions in $\text{In}_x\text{Ga}_{1-x}\text{As}$ and $\text{InAs}_x\text{P}_{1-x}$ grown from In solution at constant temperature

Journal of Applied Physics (November 2003)

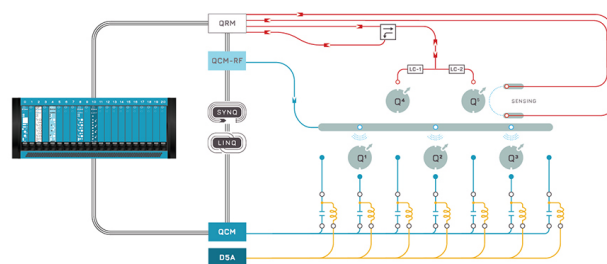
Raman scattering from $\text{In}_x\text{Ga}_{1-x}\text{As}/\text{GaAs}$ strained-layer superlattices

Appl. Phys. Lett. (April 1991)



Integrates all
Instrumentation + Software
for Control and Readout of

Superconducting Qubits
NV-Centers
Spin Qubits



Spin Qubits Setup

[find out more >](#)

Strain mapping in [111] and [001] InGaAs/GaAs superlattices

U. D. Venkateswaran, L. J. Cui, M. Li, and B. A. Weinstein
Department of Physics, SUNY at Buffalo, Buffalo, New York 14260

K. Elcess and C. G. Fonstad
Massachusetts Institute of Technology, Cambridge, Massachusetts 02139

C. Mailhot
Xerox Webster Research Center, Webster, New York 14580

(Received 21 August 1989; accepted for publication 7 November 1989)

Raman area maps measuring the strain in lattice-mismatched [111] and [001] oriented $\text{In}_x\text{Ga}_{1-x}\text{As}/\text{GaAs}$ superlattices ($x = 0.1, 0.17$) are presented and compared with independent x-ray rocking curve studies of the average strain in the same samples. We find that the LO phonon frequency, but not the TO frequency, is a valid measure of strain for [111] oriented superlattices exhibiting one-mode behavior. This is explained by the lack of compensation between the effects of alloying and strain for the TO mode in $\text{In}_x\text{Ga}_{1-x}\text{As}$. The capability to nondestructively map small growth variations in superlattice and buffer layer constituents is demonstrated.

Strained-layer superlattices (SLSLs) are receiving considerable attention due to their tailorable electronic and optoelectronic properties.¹ An intriguing example of this is the occurrence of piezoelectric fields in [111] oriented SLSLs. This effect, first predicted by Smith and Mailhot² and subsequently supported by optical^{3,4} and infrared⁵ experiments, makes possible novel nonlinear optical and electro-optical applications.

A recurrent problem for the characterization of mismatched heterostructures is the accurate measurement of the internal strains. Of the various techniques available,⁶⁻⁸ Raman scattering has the advantages of rapid, nondestructive, and spatially local measurement of the elastic strains in different constituents. Consequently, Raman scattering is potentially useful for producing areal strain maps of macroscopic films.

Previous Raman studies of strain in mismatched heterostructures have concentrated on [001] oriented films and multilayers in nonmapping applications.⁸ This letter presents Raman area maps showing subtle macroscopic variations of strain in [111] and similar [001] oriented $\text{In}_x\text{Ga}_{1-x}\text{As}/\text{GaAs}$ SLSLs. Comparison to x-ray rocking curve (XRC) measurements on the same samples,⁹ reveals that for this materials system only LO-derived data accurately describe the internal strains.

The elastic strains within the layers of a SLSL can be extracted from phonon frequency measurements by a theory originally developed to treat applied uniaxial stress.¹⁰ The expressions relating the in-plane strain ϵ_p to the induced frequency changes of the one-phonon peaks allowed in backscattering for [001] and [111] growth axes are

$$\begin{aligned} \left(\frac{\Delta\omega}{\omega}\right)_{\text{LO}} &= \frac{1}{2} [(\tilde{K}_{11} + 2\tilde{K}_{12}) \\ &\quad - \tilde{K}_{11}(1 + \Gamma)]\epsilon_p, \quad [001]\text{ growth}, \quad (1) \\ \left(\frac{\Delta\omega}{\omega}\right)_{(110)} &= \frac{1}{6} [(\tilde{K}_{11} + 2\tilde{K}_{12})(2 - \Gamma) \\ &\quad + \left(\frac{-4}{+2}\right)\tilde{K}_{44}(1 + \Gamma)]\epsilon_p, \quad [111]\text{ growth}. \quad (2) \end{aligned}$$

Here the \tilde{K}_{ij} give the strain variation of the spring constants, and Γ relates the in-plane and normal strain components according to $\epsilon_n = -\Gamma\epsilon_p$,

$$\Gamma = 2C_{12}/C_{11}, \quad [001]\text{ growth}, \quad (3)$$

$$\Gamma = 2 \frac{(C_{11} + 2C_{12} - 2C_{44})}{C_{11} + 2C_{12} + 4C_{44}}, \quad [111]\text{ growth}, \quad (4)$$

where the C_{ij} are elastic constants. Equations (1)–(4) are to be applied separately to each constituent of a SLSL. The \tilde{K}_{ij} and C_{ij} for $\text{In}_x\text{Ga}_{1-x}\text{As}$ are obtained by scaling measured values linearly between $x = 0$ and $x = 1$.⁸

The three $\text{In}_x\text{Ga}_{1-x}\text{As}/\text{GaAs}$ SLSLs studied here were grown by molecular beam epitaxy and characterized by non-Raman methods as described elsewhere.^{4,11} Their parameters were 20 periods of $\text{In}_x\text{Ga}_{1-x}\text{As}/\text{GaAs}$ layers (70 ± 5)/(140 ± 5) Å thick, buffered to semi-insulating GaAs substrates; the buffer regions were designed for “free-standing” growth. The SLSL orientations and In concentrations were for sample 1: [001] and $x = 0.1 \pm 0.02$; for sample 2: [111]B and $x = 0.1 \pm 0.02$; and for sample 3: [111]B and $x = 0.17 \pm 0.02$. Samples 1 and 2 were grown simultaneously.

Raman backscattering was excited with ≤ 20 mW of 4825 Å Kr^+ laser radiation focused into a ~ 10 - μm -diam spot, and was recorded by a scanning Raman microprobe under microcomputer control with a Si array detector. Phonon peak frequencies were located to ± 0.3 cm^{-1} accuracy by fitting the Raman lines to Lorentzian profiles. No heating-induced phonon shifts could be observed in our 300 K experiments for laser powers < 25 mW. The sample x - y position could be controlled to ± 0.5 μm in the laser focal plane. Spectra were recorded in three-point spatial clusters, with 30 μm between points and ~ 1.0 mm between clusters. Higher density mapping, though no more complicated in principle, presents nontrivial memory requirements for standard microcomputer-based systems (e.g., ~ 500 megabytes to map a 1 cm^2 area with uniform 10 μm resolution.)

We find for all the samples that the Raman spectra closely obey bulk-like backscattering selection rules. This is shown for the [111] growth case in Fig. 1. Scattering from

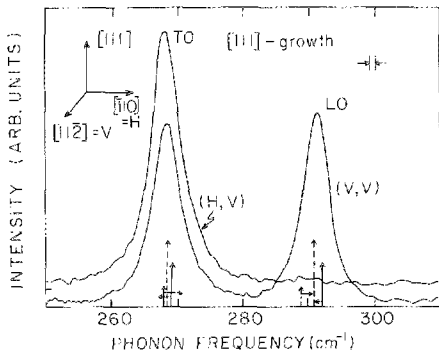


FIG. 1. Observed polarized Raman spectra for [111] oriented $\text{In}_{0.1}\text{Ga}_{0.9}\text{As}/\text{GaAs}$ SLSL showing bulk-like selection rules. Horizontal arrows show the predicted misfit-induced shifts from the unstrained frequencies (vertical solid arrows) of each SL constituent; dashed arrows locate the resulting peak centroids.

interface and higher order confined modes, which obeys different selection rules,⁸ does not contribute appreciably to our spectra. This is to be expected for the relatively thick-layer superlattices and nonresonant excitation of this study.

Although the superlattices contain two distinct chemical species, we observe only a single GaAs-like LO peak (for [001] orientation) or a single GaAs-like LO-TO pair (for [111] orientation), each at frequencies (ω_{LO} and ω_{TO}) shifted from their bulk unstrained counterparts. The appearance of single peaks is not due to poor instrument resolution. It has been explained by Iikawa *et al.* for [001] grown samples¹² as due to an exact compensation between the effects of strain and alloying in the $\text{In}_x\text{Ga}_{1-x}\text{As}$ system. We point out that such a compensation will not necessarily extend to other growth directions because the influence of strain depends both on orientation and phonon mode type. Hence, it is important to verify that this compensation applies to the [111] case at hand before a meaningful strain interpretation can proceed.

To check this, we plot in Fig. 2 the ω_{LO} and ω_{TO} of bulk unstrained $\text{In}_x\text{Ga}_{1-x}\text{As}$ alloys^{13,14} versus the misfit strain of these alloys with respect to GaAs. The solid and dashed

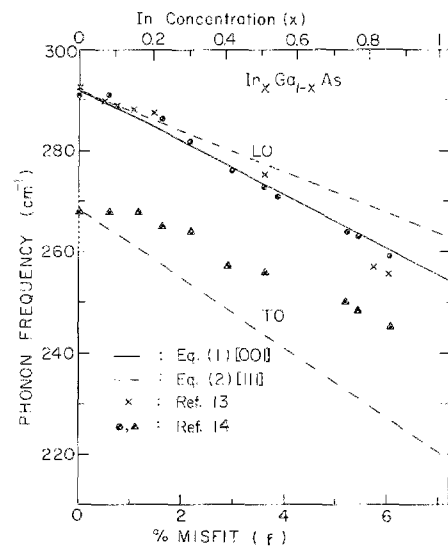


FIG. 2. Plot of the phonon frequencies in $\text{In}_x\text{Ga}_{1-x}\text{As}$ bulk alloys vs. misfit strain with respect to GaAs (bottom), and In concentration (top).

lines describe the phonon shifts predicted using Eqs. (1)–(4) for strains appropriate to [001] and [111] growth axes, respectively. The compensation between strain and alloying observed for [001] orientation is reflected in the close correspondence between the solid line and the measured ω_{LO} . Clearly, for [111] grown SLSLs a similar situation holds for the LO phonons when $f < 2\%$, i.e., $x < 27\%$. However, the compensation is not complete for the TO phonons (triangles in Fig. 2) due to the positive sign preceding \bar{K}_{44} in Eq. (2).

Figure 3 shows our internal strain maps for samples 1 and 2 ($x = 0.1$) derived from LO-Raman results. The data points are the measured spectral shifts from bulk unstrained positions rescaled to give percent in-plane strain ϵ_p via Eqs. (1)–(4). The unstrained frequencies were taken for GaAs from our own measurements, and for $\text{In}_x\text{Ga}_{1-x}\text{As}$ from a best fit (standard deviation $\pm 0.5 \text{ cm}^{-1}$) to previous data for $0 < x < 0.3$.^{13,14} An uncertainty in ϵ_p of ± 0.05 arises from our $\pm 0.3 \text{ cm}^{-1}$ peak location uncertainty. This is the main inaccuracy for mapping relative spatial variations of strain. A scale shift of similar size can also arise from the particular choice of unstrained frequencies, but this will not affect relative mapping. We find that both the samples represented in Fig. 3 exhibit small but systematic variations over macroscopic dimensions (along [110] for sample 1 and [11 $\bar{2}$] for sample 2), but appear locally uniform on a $30 \mu\text{m}$ scale.

The areal averages of the Raman measured in-plane strains for samples 1–3 obtained from the shift of both the LO and TO peaks are given in Table I along with the XRC results,⁹ and the strains expected for equivalent “free-standing” SLs. The agreement between the LO-Raman and XRC strains is excellent for samples 1 and 3, and reasonable for sample 2 (being within experimental error for GaAs but somewhat outside for InGaAs). The latter discrepancy could easily arise from the XRC fitting procedure yielding

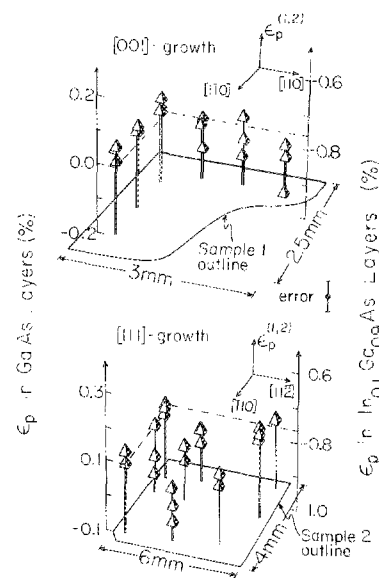


FIG. 3. LO derived area maps of the in-plane strains ϵ_p for samples 1 and 2 obtained from measured peak-shift maps according to $\epsilon_p = \Pi(\Delta\omega)_{\text{LO}}$ [see Eqs. (1) and (2)]; Π (sample 1) = 0.190, 0.199 and Π (sample 2) = 0.248, 0.262 for their respective GaAs, InGaAs layers. Left axis applies to GaAs and right axis to $\text{In}_{0.1}\text{Ga}_{0.9}\text{As}$. Error flag shows relative (point-to-point) mapping uncertainty. Dashed lines give spatially averaged strains.

TABLE I. Percent in-plane strain measured by Raman and XRC for samples 1–3 and predicted for equivalent free-standing (FS) SLSLs. Maximum uncertainties in ϵ_p are ± 0.1 for Raman and ± 0.05 for XRC. The XRC analysis gave best-fit In compositions of $x = 0.11, 0.09, 0.17$ for samples 1, 2, and 3, respectively.

Sample No.	ϵ_p [GaAs]			ϵ_p [In _x Ga _{1-x} As]		
	Raman	XRC	FS	Raman	XRC	FS
1	-0.004(LO)	0.007	0.26	-0.76(LO)	-0.77	-0.53
2	0.10(LO)	0.14	0.22	-0.76(LO)	-0.51	-0.43
	0.07(TO)			-0.12(TO)		
3	0.30(LO)	0.33	0.41	-0.96(LO)	-0.93	-0.82
	0.18(TO)			-0.16(TO)		

too small an x value, or from variations of the In content at depths exceeding the ~ 2000 Å laser penetration. Overall we regard the independent agreement between the LO–Raman and XRC strains to be quite satisfactory, and of equal quality for the [001] and [111] grown samples. The latter comparison is a consistency check supporting our (orientation independent) choice of the unstrained reference frequencies.

In contrast, the TO–Raman-derived strains show a clear trend toward smaller values, deviating from both the XRC and the LO phonon results, especially for the InGaAs layers. The strain underestimate arises because, unlike LO, the shift (see Fig. 2) of the bulk TO frequency with alloying is considerably weaker than that due to strain. This causes the centroid of the TO peak (which contains phonon contributions from both SL constituents) to end up closer to either bulk reference frequency than warranted by strain. (See the arrows in Fig. 1.)

That this occurs without substantial broadening of the single symmetric TO peak (compared to LO) is not altogether unexpected. Single peak behavior is an interesting property of the In_xGa_{1-x}As/GaAs system which has been observed repeatedly in [001] grown samples for $x < 0.2$,^{8,12,13} as well as in the present [111] oriented $x = 0.1, 0.17$ SLSLs. Although not completely understood, it is related to the frequency overlap between the *internal-strain-shifted* GaAs-like optic branches in each SL constituent.⁸ Even for incomplete strain alloying compensation, one can have sufficient degeneracy within the Raman peak width to suppress the occurrence of spatially modulated frequencies. For example, the strain-shifted ω_{TO} of GaAs and In_{0.17}Ga_{0.83}As differ by only ~ 6 cm⁻¹ compared to the 5.5 cm⁻¹ Raman width. The range of q -scattered needed to include chemical disorder, structural disorder, and thermal decay determines the frequency overlap. As these effects are not easily separated even in bulk In_xGa_{1-x}As, which exhibits one-mode behavior for $x < 0.27$,¹⁴ further study of the SLSLs, perhaps by applied uniaxial stress, would be helpful.

Table I allows an assessment of several sample characteristics related to growth. In each of the SLSLs the measured GaAs strains are lower than what is expected for free-standing growth, indicating that the graded buffer layers may be In deficient. This is consistent with secondary-ion mass spectroscopy and Rutherford backscattering studies on sections from the same parent SLSLs.⁴ For pseudomorphic growth of elastically similar materials, ϵ_p is expected to be¹

$$\epsilon_p^{(1,2)} = \pm [h^{(2,1)}/(h^{(1)} + h^{(2)})]f + \bar{\epsilon}_s, \quad (5)$$

where superscripts (1,2) label the constituents, h is the layer width, f is the bulk misfit, and $+$ applies to constituent (1) (here GaAs). The first term on the right is the strain for a free-standing SL, and $\bar{\epsilon}_s$ is the net residual strain due to the substrate, or buffer in our case.

$\bar{\epsilon}_s$ was computed from the measured $\epsilon_p^{(1,2)}$ assuming the individual SL layers did not exceed their critical thickness h_c , normally ~ 1500 Å for In_{0.1}Ga_{0.9}As films on GaAs.¹³ We find that $\bar{\epsilon}_s \leq -0.25\%$ for each SLSL. This is small compared to the maximum absolute misfits of 0.72% and 1.22% for our $x = 0.1$ and $x = 0.17$ samples, respectively. Hence, by any current estimates,¹ the 4200 Å thickness of these SLSLs should not exceed pseudomorphic limits. Very recent transmission electron microscopy characterization showing that threading dislocations are well confined to the buffer regions bears this out.⁴

In conclusion, LO Raman scattering is an effective technique for mapping the internal strain in [111] and [001] oriented In_xGa_{1-x}As/GaAs SLSLs. However, comparison to XRC data shows that TO scattering should not be used because strain alloying compensation does not apply for TO as it does for LO. Evidence for pseudomorphic growth, with some net compression and macroscopic inhomogeneities, was found in the [001] and the piezoelectric [111] SLSLs mapped in the present study.

The authors thank C. R. Wie and H. M. Kim for providing XRC data prior to publication, and D. L. Smith and B. K. Laurich for helpful discussions. Work at SUNYAB was partially supported by Xerox WRC, ONR grant No. N00014-89-J1797, and the University CEEM center. Work at MIT was supported by NSF grant No. DMR84-18718 through the MS&E center.

¹See, for example, E. P. O'Reilly, *Semicond. Sci. Technol.* **4**, 121 (1989); G. C. Osbourn, *J. Vac. Sci. Technol. B* **1**, 379 (1983).

²D. L. Smith and C. Mailhot, *Phys. Rev. Lett.* **58**, 1264 (1987); C. Mailhot and D. L. Smith, *Phys. Rev. B* **35**, 1242 (1987).

³B. K. Laurich, K. Elcess, C. G. Fonstad, J. G. Beery, C. Mailhot, and D. L. Smith, *Phys. Rev. Lett.* **62**, 649 (1989).

⁴J. G. Beery, B. K. Laurich, C. J. Maggiore, D. L. Smith, K. Elcess, C. G. Fonstad, and C. Mailhot, *Appl. Phys. Lett.* **54**, 233 (1989); D. L. Smith and B. K. Laurich (private communications).

⁵B. S. Yoo, X. C. Liu, A. Petrou, J. P. Cheng, A. A. Reeder, B. D. McCombe, K. Elcess, and C. G. Fonstad, *Superlatt. Microstruct.* **5**, 363 (1989).

⁶W. K. Chu, J. A. Ellison, S. T. Picraux, R. M. Biefeld, and G. C. Osbourn, *Phys. Rev. Lett.* **52**, 125 (1984).

⁷C. R. Wie, T. A. Tombrello, and T. Vreeland, Jr., *J. Appl. Phys.* **59**, 3743 (1986).

⁸M. Cardona, and G. Güntherodt, eds., "*Light Scattering in Solids V*," *Topics in Applied Physics*, Vol. 66 (Springer, New York, 1989), Chap. 3 and references therein.

⁹H. M. Kim, C. R. Wie, K. Elcess, and C. G. Fonstad, *Proceedings of the Materials Research Society*, Boston, MA, 1989; private communications.

¹⁰F. Cerdeira, C. J. Buchenauer, F. H. Pollak, and M. Cardona, *Phys. Rev. B* **5**, 580 (1972).

¹¹K. Elcess, J. L. Ljevin, and C. G. Fonstad, *J. Vac. Sci. Technol. B* **6**, 638 (1988).

¹²F. Iikawa, F. Cerdeira, C. Vazquez-Lopez, P. Motisuke, M. A. Sacilotti, A. P. Roth, and R. A. Masut, *Solid State Commun.* **68**, 211 (1988).

¹³G. Burns, C. R. Wie, F. H. Dacol, G. D. Pettit, and J. M. Woodall, *Appl. Phys. Lett.* **51**, 1919 (1987).

¹⁴G. Lucovsky and M. F. Chen, *Solid State Commun.* **8**, 1397 (1970).